Cambrian (?) Mill Creek diabase dike swarm, eastern Arbuckles: A Glimpse of Cambrian rifting in the Southern Oklahoma Aulacogen

Edward G. Lidiak[1], Rodger E. Denison[2], and Robert J. Stern[3]

[1]*Department of Geology and Planetary Science, University of Pittsburgh, Pittsburgh, Pennsylvania 15260. egl@pitt.edu. Corresponding author.*

[2]*15141 Kingstree Drive, Dallas, Texas 75248. redenison@aol.com.*

[3]*Department of Geosciences, The University of Texas at Dallas, Box 830688, Richardson, Texas 75083-0688. rjstern@utdallas.edu.*

ABSTRACT

A swarm of Cambrian (?) diabase dikes intrude the 1390-1365 Ma granitoids of the eastern Arbuckle Mountains of Oklahoma. The dikes strike predominantly N60°W parallel to the rifted margin of the Southern Oklahoma Aulacogen and are interpreted as being related to Cambrian opening of that structure. The dikes, referred to here as the Mill Creek diabases, are olivine-normative to quartz-normative tholeiitic basalts. Their tholeiitic character is further indicated by high $Fe_2O_3^T$ (total Fe), moderate to high TiO_2, low P_2O_5, and low Nb/Y ratio. Mg numbers (Mg#) of 52-36 are indicative of derivative basaltic liquids which are consistent with the fine-grained, equigranular mineral assemblage of plagioclase + augite + Fe-Ti oxides ± olivine of most diabases.

The timing and tectonic setting of the diabases suggest that they were intruded in association with the Early Cambrian break-up of the southern Laurentian supercontinent. These dikes testify to the probable existence and subsequent break-up of a large igneous province (LIP) in this region and demonstrate that Cambrian LIPs were compositionally similar to better-known break-up LIPs of Mesozoic and younger age. This occurrence is the only evidence that we can find for the presence of a break-up LIP in southern Laurentia, but we argue that compositional similarities with other, better preserved LIPs warrant the conclusion that the Cambrian break-up LIP of the southern mid-continent was similarly extensive.

INTRODUCTION

The Southern Oklahoma Aulacogen (SOA) is a well-known transverse structure that trends west-northwest in the southern North American craton. Exposures within the SOA reveal faults that record extension and which may be interpreted as related to its formation. Mesoproterozoic basement underlies much of the region and ~1390 Ma gneiss and granodiorite and ~1365 Ma granite are exposed in the eastern Arbuckle Mountains (Figures 1, 2). Diabase dikes are widespread throughout the core of the eastern Arbuckles. These dikes are referred to here as the Mill Creek diabase dike swarm for excellent exposures in Mill Creek Quarry (Figures 2, 3), which is here designated as the type locality. In the quarry, a swarm of steeply dipping diabase dikes (from <1 m to several meters wide) intrudes the Troy Granite. The dikes strike predominantly west-northwest and may have been intruded along fractures co-genetic with faulting and Cambrian deformation. We interpret these dikes as being emplaced during formation of the SOA and part of the Southern Oklahoma Aulacogen Large Igneous Province (SOA–LIP) (Lidiak et al., 2005; Hanson et al., 2011, 2013). In addition, a number of diabase dikes may have been emplaced earlier, apparently about the time that the Mesoproterozoic granitoids formed. These dikes, along with a suite of silicic west-northwest-trending microgranite porphyry dikes, record a Mesoproterozoic structural trend that influenced Paleozoic structure. Dikes from the two diabase suites cannot be easily distinguished petrographically but have distinct geochemical signatures as discussed below.

The Mill Creek diabase dike swarm occurs along the present northern margin of the SOA (Figure 1). Similar Cambrian diabase dikes crop out about 200 km to the west

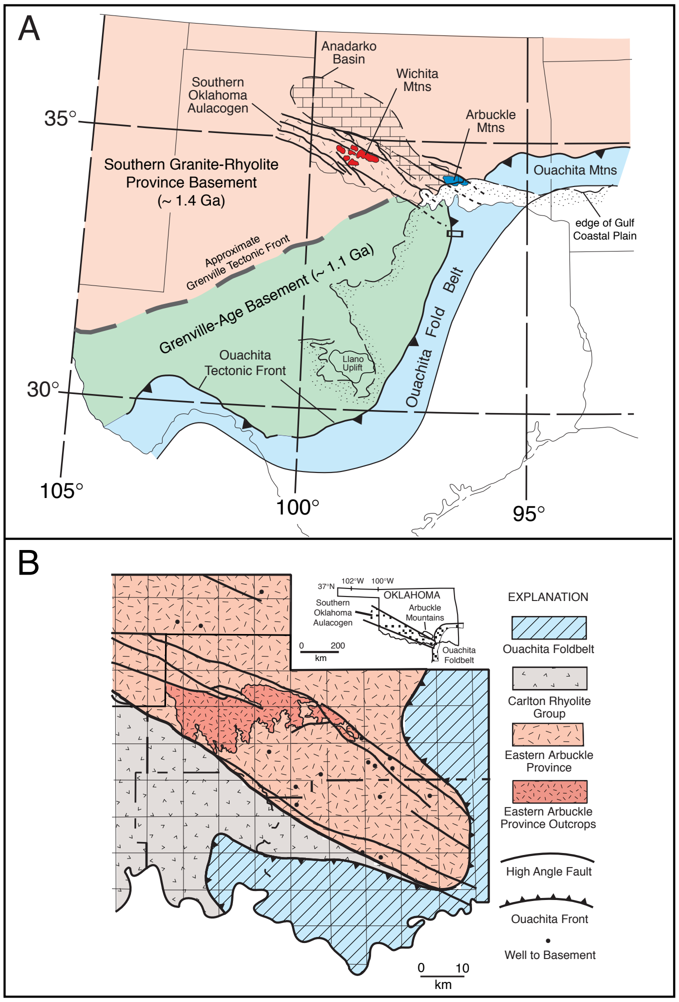

Figure 1: A) Generalized tectonic map of Texas and adjacent regions of Oklahoma and New Mexico. Base map and Phanerozoic structures adapted from Viele and Thomas (1989) with additions from Ham et al. (1964). Precambrian boundaries and provinces adapted from (Ewing (1990, 1991) and Van Schmus et al. (1993). B) Main tectonic elements of southeastern Oklahoma adapted from Ham et al. (1964).

in the Wichita Mountains (Gilbert, 1982, 1983; Price et al., 1996) and are present in the subsurface within the confines of the SOA (Ham et al., 1964; Puckett, 2011; Puckett et al., 2011). In the eastern Arbuckles, Phanerozoic sedimentary rocks lie unconformably on the basement, testifying to a significant amount of erosion after dike emplacement. The dike rocks are fine grained, suggesting that the present level of exposure corresponds to an emplacement depth of only a km or so beneath the Cambrian surface. Dike contacts are sharp and rare xenoliths of granite show no reaction with diabase; these two observations suggest that there was little contamination by the surrounding country rocks. These dikes must have fed a volcanic field but there are no known basalt flows associated with the Mill Creek diabase dike swarm.

REGIONAL SETTING

The late Neoproterozoic-Cambrian continental margin in the southern and eastern North American craton formed in a passive-margin tectonic setting in which carbonate-shelf facies and rifted-margin basins developed during the initial opening of the Iapetus Ocean (Rankin, 1976; Rankin et al., 1989; Thomas, 1989, 1993; Viele and Thomas, 1989; Harry and Londono, 2004). This extensional episode was accompanied in the Appalachians (Rankin, 1976) and in the SOA (Gilbert, 1983) by extensive magmatism. In the Appalachians there were two main episodes of magmatism at 615 to 564 Ma and at about 550 to 540 Ma (Cawood et al., 2001; Puffer, 2002). In east-central Mexico a mafic dike swarm records a separation date of 546 Ma (Keppie et al., 2006). Mafic igneous activity in the Wichitas is approximately 10 to 20 Ma younger but is well constrained at 534 to 528 Ma (Lambert et al., 1988; Hogan et al., 1995, 1996; Hames et al., 1998). These dates record the initial stages of rifting along the southern margins of the Laurentian craton. The rifting associated with the SOA is best exposed in southern Oklahoma (Figure 1), but this rifting episode affected regions far to the west-northwest across the Texas Panhandle and into Colorado (Hansen and Peterman, 1968; Olson et al., 1977). Detailed mapping in the Precambrian basement of the eastern Arbuckles (Denison, 1973) documents the abundance of N60°W-striking diabase dikes. A rose diagram (Denison, 1982, 1995) and later measurements show the trend of 365 diabase dikes as measured in the field (Figure 4). This trend parallels the late Paleozoic structural direction of about N60°W, and we speculate that Ediacaran-Cambrian “SOA” rift structures may have controlled the development of Late Paleozoic “Ouachita” structures.

AGES OF INTRUSION

Table 1 lists available K-Ar whole rock dates for eastern Arbuckle diabase dikes (Denison, unpublished Mobil data). Three of the ten dates are in the expected ~500 Ma age range, and two others are ~1300 Ma. The other five samples give dates of 748, 795, 1098, 1532, and 2074 Ma; these dates do not correspond to ages of rocks in the Ar-

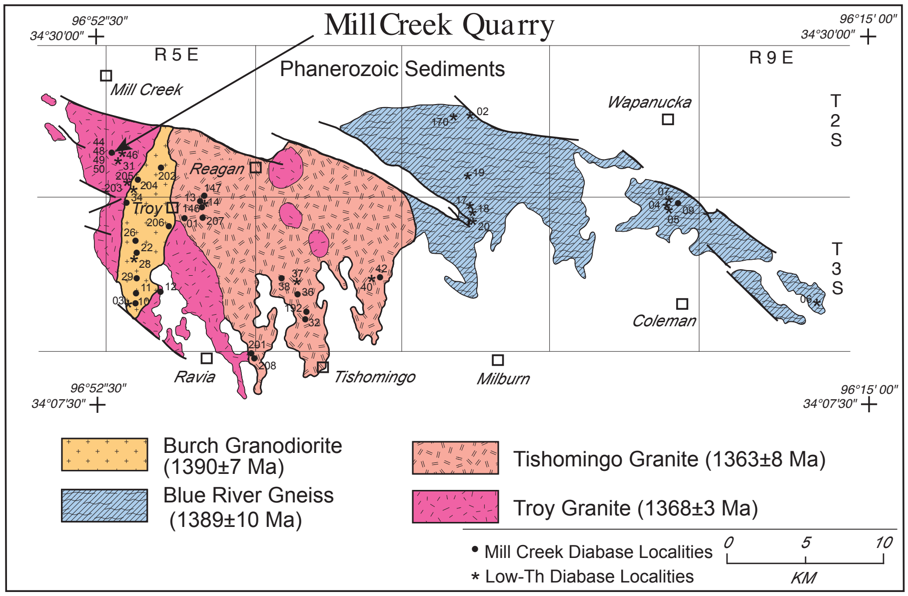

Figure 2: Geologic map of Precambrian rocks of the eastern Arbuckle Mountains, Oklahoma (Denison, 1973), showing location of Mill Creek Quarry and location of eastern Arbuckle diabase samples studied in this report. Detailed sample localities are listed in Appendix 1.

buckles and may be too old, due to inherited ^{40}Ar, or too young, due to ^{40}Ar loss. A concerted effort to extract and date zircons and/or baddeleyite from these dikes, as well as efforts to obtain reliable ^{40}Ar/^{39}Ar ages, is critically needed in order (1) to determine exactly when the inferred Cambrian (Mill Creek) dikes were emplaced in the SOA and (2) to test the idea that some of these Arbuckle diabase dikes are significantly older than Cambrian.

A Cambrian age of the Mill Creek diabases is suggested by the fact that diabase dikes in both the Arbuckle and Wichita areas cut the voluminous felsic volcanics of the Cambrian Carlton Rhyolite Group (Ham et al., 1964; Gilbert and Hughes, 1986; Hogan et al., 1998). These dikes represent the culmination of Cambrian igneous activity in the SOA. In addition, at least another episode of diabase dike intrusion in the eastern Arbuckles is

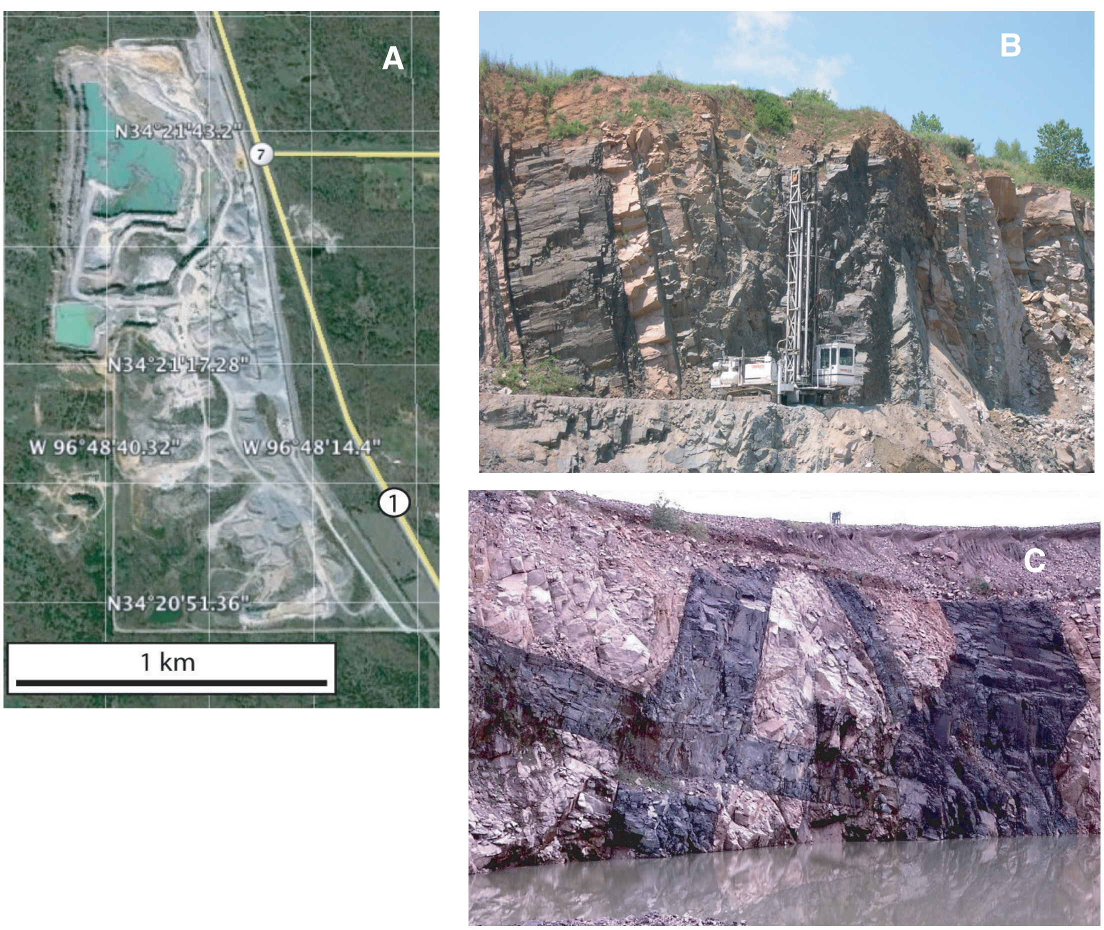

Figure 3: A) Google Earth image of Mill Creek Quarry. B) Photograph in the quarry of exposed dikes (dark) intruding Mesoproterozoic Troy Granite (light). C) Photograph in the quarry of cross-cutting diabase dikes.

TABLE 1: SUMMARY OF K-AR AGES FOR EASTERN ARBUCKLE DIABASE DIKES

ARBUCKLE DIABASE DATES

Sample #	%K	Sample type	Age (Ma)	Location
1431	0.225	whole rock	1532	C NE 3-3S-5E, ca.100 yards south of Capitol quarry
1432	0.393	whole rock	538	NE SW NE 3-3S-5E at Rock Creek crossing
1459	0.280	whole rock	795	SW SW SE SW 2-2S-5E cuts Troy Granite
1461	0.374	whole rock	1324	C NE SW 28-3S-6E Harris quarry dike
1464	0.477	whole rock	594	NW SE SW 28-3S-6E cuts Tishomingo Granite
1474	0.360	whole rock	506	NW SE NW 1-3S-8E
1486	0.555	whole rock	748	C W1/2 SE SW 28-3S-6E
1491	0.195	whole rock	1332	C SL SW SE 16-2S-7E
1504	0.190	whole rock	2074	NW NW NW 27-2S-5E
1507	0.280	whole rock	1098	C NL NW NE 19-2S-5E

indicated by cross-cutting diabase dikes in the Mill Creek Quarry (Figure 3C) and by the presence of two distinct geochemical suites within the diabases (discussed below). Indirect evidence for a significantly older (Precambrian?) age of one of the suites is suggested by a K–Ar date of 1291±26 Ma (Denison, unpublished Mobil data) on biotite from the Tishomingo Granite that is immediately adjacent to a 5-m-thick diabase dike in the Harris Quarry (Taylor, 1915). If this dike were Cambrian in age, the K–Ar date should be partially reset.

PETROGRAPHY AND MINERALOGY

The diabases are fine-grained rocks composed mostly of plagioclase, clinopyroxene, and Fe–Ti oxides with or without olivine. Sphene, hornblende, biotite, quartz and potash feldspar are found locally as trace minerals. Apatite is a ubiquitous accessory mineral. Alteration minerals chlorite, calcite, epidote, sericite, clays and zeolites are common. The average grain size varies from 5 mm to 0.05 mm depending on the dike thickness and proximity to the margin. The texture varies from ophitic to subophitic to intersertal. Microamygdules are common in some dikes.

Plagioclase is invariably lath shaped and rarely occurs as phenocrysts. Microprobe analyses show that the composition ranges from calcic andesine (An_{47}) to labradorite (An_{57}–An_{59}) depending on the bulk composition of the rock. Andesine is most common in dikes with quartz and potash feldspar. Labradorite is characteristic of olivine-bearing diabases. Twinning is well defined. Sericite and lesser clays mottle the plagioclase in most dikes.

Clinopyroxene is generally a brownish to purple-tinted augite. A representative microprobe composition is $Wo_{36}En_{42}Fs_{22}$. The augite forms large ophitic hosts for the plagioclase laths as well as smaller interlath crystals. Clinopyroxene mostly alters to chlorite although actinolite is locally common.

Microprobe analyses of Fe-Ti oxides indicate that both magnetite and ilmenite are present. The oxides vary from rounded granular shapes to highly angular crystals. The angular shapes are more common in diabases showing ophitic textures. Iron sulfides make up a significant percent of the opaque minerals in some diabases.

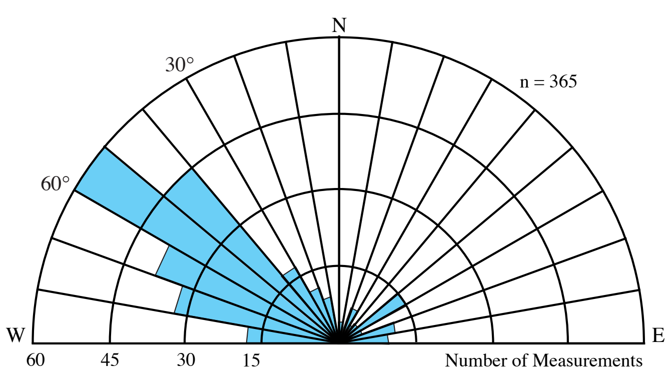

Figure 4: Rose diagram showing strike direction of diabase dikes, eastern Arbuckle Mountains, Oklahoma (Denison, 1995).

ANALYTICAL TECHNIQUES

Twenty-eight samples of representative Mill Creek diabases were selected for major- and trace-element analyses. An additional eighteen samples of low-Th, presumably older, diabases were also analyzed for trace-elements compositions. All samples were prepared for analysis by crushing to 200-mesh in a steel mortar. Both major and trace elements were analyzed at the Centre for Earth Resources Research, Department of Earth Sciences, Memorial University of Newfoundland. Major elements were analyzed by X-ray fluorescence (XRF) using fused lithium metaborate-lithium tetraborate glass beads. Trace elements were analyzed by inductively coupled plasma mass spectrometry. The procedures are described elsewhere (Longerich et al., 1990). The analyses were run twice and compared with XRF data from the samples and from measured values of standard reference materials. The results of the major- and trace-element analyses of the Mill Creek samples are listed in Tables 2 and 3, respectively. The low-Th diabases are listed in Table 4. $^{87}Sr/^{86}Sr$ was determined using the Finnigan MAT 261 solid-source mass spectrometer at the University

TABLE 2. MAJOR ELEMENTS AND CIPW NORMS, MILL CREEK DIABASE DIKES, EASTERN ARBUCKLE MOUNTAINS

Oxide	Arb-01	Arb-09	Arb-10	Arb-11	Arb-11[1]	Arb-12	Arb-13	Arb-14	Arb-22	Arb-26	Arb-29	Arb-32	Arb-32[1]	Arb-34	Arb-36	Arb-37	Arb-42	Arb-44	Arb-48	Arb-49a
SiO_2	48.60	48.20	47.89	46.19	46.50	49.13	49.32	48.54	51.86	46.70	46.96	49.11	48.80	49.26	48.70	50.38	49.49	49.47	49.51	50.23
TiO_2	2.34	2.38	2.14	2.59	2.51	2.13	2.15	2.14	2.20	2.71	1.96	2.54	2.49	2.13	2.32	1.85	2.24	2.33	2.24	2.87
Al_2O_3	13.40	13.48	13.67	14.03	14.20	14.03	13.96	13.96	13.50	14.50	15.67	13.70	13.90	13.95	14.70	13.78	13.48	13.28	14.83	14.09
$Fe_2O_3^T$	14.90	15.32	13.46	15.55	15.10	14.07	14.14	14.98	14.75	14.77	13.36	14.65	14.50	14.27	13.86	14.19	13.58	14.54	14.80	15.40
MgO	6.10	6.22	7.07	6.17	6.25	6.57	6.48	5.79	4.26	4.84	7.04	5.64	5.54	6.56	4.98	5.22	6.15	4.43	6.52	6.22
MnO	0.19	0.19	0.19	0.21	0.20	0.19	0.18	0.21	0.20	0.17	0.19	0.19	0.17	0.18	0.20	0.21	0.19	0.23	0.21	0.20
CaO	11.20	8.80	11.69	9.38	9.28	10.45	10.43	9.33	7.10	8.22	9.11	9.65	9.54	10.39	6.40	9.43	9.76	8.25	9.81	9.23
Na_2O	2.15	2.87	1.58	2.72	2.67	2.25	2.19	2.98	3.14	2.81	2.88	2.73	2.68	2.25	3.84	2.36	2.33	3.05	2.31	2.61
K_2O	0.34	1.22	0.45	0.79	0.75	0.59	0.57	0.84	1.58	1.17	0.84	0.94	0.89	0.58	0.93	0.77	1.04	1.76	0.70	0.75
P_2O_5	0.23	0.30	0.28	0.39	0.35	0.22	0.23	0.28	0.36	0.65	0.33	0.47	0.42	0.22	0.59	0.24	0.27	0.67	0.24	0.37
LOI	0.23	0.91	1.11	1.84	1.95	0.26	0.16	0.68	0.99	2.55	1.49	0.58	0.55	0.24	2.52					
Total	99.68	99.89	99.53	99.86	99.76	99.89	99.81	99.73	99.94	99.09	99.83	100.20	99.48	100.03	99.04	98.43	98.53	98.01	101.17	101.97
Mg#	44.8	44.6	51.0	44.0	45.1	48.1	47.6	43.4	36.4	39.4	51.1	43.3	43.1	47.7	41.6	42.2	47.3	37.6	46.6	44.5

[1] duplicate analysis
[2] East Timber Hills diabase dikes (Eschberger et al., this volume)
[3] Rhyolite Porphyry (Carlton Rhyolite?)

Major Element Compositions - Normalized to 100% Anhydrous

Oxide	Arb-01	Arb-09	Arb-10	Arb-11	Arb-11[1]	Arb-12	Arb-13	Arb-14	Arb-22	Arb-26	Arb-29	Arb-32	Arb-32[1]	Arb-34	Arb-36	Arb-37	Arb-42	Arb-44	Arb-48	Arb-49a
SiO_2	48.87	48.70	48.66	47.12	47.54	49.31	49.49	49.01	52.41	48.37	47.75	49.30	49.33	49.38	50.46	51.18	50.23	50.47	48.92	49.25
TiO_2	2.35	2.40	2.17	2.64	2.57	2.14	2.16	2.16	2.22	2.81	1.99	2.55	2.52	2.14	2.40	1.86	2.27	2.38	2.21	2.81
Al_2O_3	13.47	13.62	13.89	14.31	14.52	14.08	14.01	14.09	13.64	15.02	15.93	13.75	14.05	13.98	15.23	13.86	13.68	13.55	14.65	13.81
$Fe_2O_3^T$	14.98	15.48	13.68	15.86	15.44	14.12	14.19	15.12	14.91	15.30	13.59	14.71	14.66	14.30	14.36	14.27	13.78	14.84	14.62	15.10
MgO	6.13	6.28	7.18	6.29	6.39	6.59	6.50	5.85	4.31	5.01	7.16	5.66	5.60	6.58	5.16	5.25	6.24	4.52	6.44	6.10
MnO	0.19	0.19	0.19	0.21	0.20	0.19	0.18	0.21	0.20	0.18	0.19	0.19	0.17	0.18	0.21	0.21	0.19	0.23	0.21	0.20
CaO	11.26	8.89	11.88	9.57	9.49	10.49	10.47	9.42	7.18	8.51	9.26	9.69	9.64	10.41	6.63	9.48	9.91	8.42	9.69	9.05
Na_2O	2.16	2.90	1.61	2.77	2.73	2.26	2.20	3.01	3.17	2.91	2.93	2.74	2.71	2.26	3.98	2.37	2.36	3.11	2.28	2.56
K_2O	0.34	1.23	0.46	0.81	0.77	0.59	0.57	0.85	1.60	1.21	0.85	0.94	0.90	0.58	0.96	0.77	1.06	1.80	0.69	0.74
P_2O_5	0.23	0.30	0.28	0.40	0.36	0.22	0.23	0.28	0.36	0.67	0.34	0.47	0.42	0.22	0.61	0.24	0.27	0.68	0.24	0.36
Total	100	100	100	100	100	100	100	100	100	100	100	100	100	100	100	100	100	100	100	100

CIPW Norms (normalizing fators: total oxides = 100%; Fe^{+3}/(total Fe) = 0.15)

Norm	Arb-01	Arb-09	Arb-10	Arb-11	Arb-11[1]	Arb-12	Arb-13	Arb-14	Arb-22	Arb-26	Arb-29	Arb-32	Arb-32[1]	Arb-34	Arb-36	Arb-37	Arb-42	Arb-44	Arb-48	Arb-49a
Qtz	1.37	0.00	1.66	0.00	0.00	0.64	1.37	0.00	3.10	0.00	0.00	0.00	0.16	0.80	0.00	4.32	1.32	0.00	0.34	1.20
Plag	44.33	45.05	42.94	47.66	48.19	45.65	45.28	47.89	45.09	48.97	52.60	45.63	46.44	45.41	54.53	44.96	43.57	44.01	46.99	45.67
Or	2.01	7.27	2.72	4.79	4.55	3.49	3.37	5.02	9.46	7.15	5.02	5.56	5.32	3.43	5.67	4.55	6.26	10.64	4.08	4.37
Di	23.44	17.92	22.82	17.10	16.25	19.85	19.61	18.67	12.58	11.24	13.08	18.70	17.88	19.74	6.69	17.11	19.63	16.42	15.54	15.34
Hy	19.31	10.97	20.95	8.94	11.88	21.51	21.43	12.36	20.21	18.12	6.21	19.57	19.99	21.75	18.39	20.15	20.10	17.80	23.83	22.67
Ol	0.00	8.85	0.00	10.75	8.75	0.00	0.00	6.74	0.00	2.99	14.40	0.16	0.00	0.00	4.39	0.00	0.00	0.54	0.00	0.00
Il	4.46	4.56	4.12	5.01	4.88	4.06	4.10	4.10	4.22	5.34	3.78	4.84	4.79	4.06	4.56	3.53	4.31	4.52	4.20	5.34
Mt	3.26	3.36	2.97	3.45	3.36	3.07	3.09	3.29	3.25	3.32	2.96	3.20	3.19	3.12	3.12	3.10	3.00	3.23	3.18	3.28
Ap	0.53	0.70	0.65	0.93	0.83	0.51	0.53	0.65	0.83	1.55	0.79	1.09	0.97	0.51	1.41	0.56	0.63	1.58	0.56	0.83
Mg#	44.8	44.6	51.0	44.0	45.0	48.0	47.6	43.4	36.4	39.4	51.1	43.3	43.1	47.7	41.6	42.1	47.3	37.6	46.6	44.5

TABLE 2. MAJOR ELEMENTS AND CIPW NORMS, MILL CREEK DIABASE DIKES, EASTERN ARBUCKLE MOUNTAINS, CONTINUED

Oxide	Arb-49b	Arb-50	Arb-147	Arb-192	Arb-201	Arb-202	Arb-205	Arb-206	Arb-207	Arb-208	Mean Arb. Dbs	Std Dev	Mean ETH Diab [2]	Std Dev.	Arb-140[3]	Arb-150[3]	Arb-336[3]
SiO_2	49.33	48.43	50.30	49.29	47.00	48.76	49.01	49.28	49.50	48.24	48.80	1.24	49.30	1.50	72.82	73.14	72.38
TiO_2	2.93	2.70	2.01	2.11	2.84	2.42	2.25	2.30	2.01	3.40	2.37	0.34	2.07	0.25	0.59	0.57	0.53
Al_2O_3	13.26	13.30	14.26	13.49	13.70	13.87	13.90	13.78	14.54	12.50	13.89	0.58	14.81	0.94	12.83	12.91	12.73
$Fe_2O_3^T$	14.71	15.37	12.64	14.09	14.35	14.49	13.36	13.45	12.58	14.53	14.33	0.77	14.23	0.74	3.50	3.28	3.15
MgO	5.57	5.74	6.94	6.58	5.92	6.69	6.72	6.67	6.89	5.64	6.05	0.75	6.73	0.66	0.36	0.27	0.32
MnO	0.20	0.20	0.18	0.22	0.17	0.20	0.19	0.19	0.18	0.20	0.19	0.01	0.22	0.01	0.02	0.04	0.03
CaO	9.18	9.67	10.30	10.17	9.12	10.14	9.99	10.00	10.26	7.72	9.47	1.11	9.54	1.14	0.42	0.41	1.08
Na_2O	2.59	2.74	2.21	2.51	2.27	2.38	2.33	2.27	2.25	2.35	2.54	0.41	2.55	0.16	3.94	3.82	3.57
K_2O	0.73	0.82	0.45	0.47	0.67	0.52	0.56	0.53	0.47	1.20	0.80	0.33	1.62	0.58	4.67	4.70	4.75
P_2O_5	0.31	0.35	0.22	0.22	0.26	0.18	0.23	0.22	0.22	0.40	0.32	0.13	0.36	0.09	0.11	0.10	0.09
LOI		0.77		0.60	3.60	0.10	1.30	1.10	0.90	3.80	0.94	1.05	1.72	0.35	0.64	0.73	1.22
Total	98.81	100.09	99.51	99.75	99.90	99.75	99.84	99.79	99.80	99.98	99.70	0.74	103.15		99.90	99.97	99.85
Mg#	42.9	42.5	52.1	48.1	45.0	47.8	49.9	49.6	52.0	49.6	45.5	4.0	48.25		16.9	14	16.6

Major Element Compositions - Normalized to 100% Anhydrous

Oxide	Arb-49b	Arb-50	Arb-147	Arb-192	Arb-201	Arb-202	Arb-205	Arb-206	Arb-207	Arb-208	Mean Arb. Dbs	Std Dev	Mean ETH Diab [2]	Std Dev.	Arb-140[3]	Arb-150[3]	Arb-336[3]
SiO_2	49.92	48.76	50.55	49.71	48.81	48.93	49.74	49.93	50.05	50.16	49.40		48.60		73.36	73.70	73.39
TiO_2	2.97	2.72	2.02	2.13	2.95	2.43	2.28	2.33	2.03	3.54	2.40		2.04		0.59	0.57	0.54
Al_2O_3	13.42	13.39	14.33	13.61	14.23	13.92	14.11	13.96	14.70	13.00	14.07		14.60		12.93	13.01	12.91
$Fe_2O_3^T$	14.89	15.47	12.70	14.21	14.90	14.54	13.56	13.63	12.72	15.11	14.51		14.03		3.53	3.31	3.19
MgO	5.64	5.78	6.97	6.64	6.15	6.71	6.82	6.76	6.97	5.86	6.12		6.64		0.36	0.27	0.32
MnO	0.20	0.20	0.18	0.22	0.18	0.20	0.19	0.19	0.18	0.21	0.20		0.22		0.02	0.04	0.03
CaO	9.29	9.74	10.35	10.26	9.47	10.18	10.14	10.13	10.37	8.03	9.46		9.41		0.42	0.41	1.10
Na_2O	2.62	2.76	2.22	2.53	2.36	2.39	2.36	2.30	2.28	2.44	2.58		2.51		3.97	3.85	3.62
K_2O	0.74	0.83	0.45	0.47	0.70	0.52	0.57	0.54	0.48	1.25	0.81		1.60		4.70	4.74	4.82
P_2O_5	0.31	0.35	0.22	0.22	0.27	0.18	0.23	0.22	0.22	0.42	0.33		0.35		0.11	0.10	0.09
Total	100	100	100	100	100	100	100	100	100	100	100		100		100	100	100

CIPW Norms (normalizing fators: total oxides = 100%; Fe^{+3}/(total Fe) = 0.15)

Norm	Arb-49b	Arb-50	Arb-147	Arb-192	Arb-201	Arb-202	Arb-205	Arb-206	Arb-207	Arb-208	Mean Arb. Dbs	Std Dev	Mean ETH Diab [2]	Std Dev.	Arb-140[3]	Arb-150[3]	Arb-336[3]
Qtz	2.41	0.00	2.70	0.47	1.19	0.01	1.11	1.86	1.57	3.62	0.00		0.00		29.52	30.63	29.86
Plag	44.84	45.05	46.59	45.80	46.14	45.94	46.19	45.63	47.75	41.47	46.21		45.08		34.96	33.96	35.37
Or	4.37	4.90	2.66	2.78	4.14	3.07	3.37	3.19	2.84	7.39	4.78		9.46		27.78	28.01	28.48
Di	17.72	20.20	18.13	20.68	15.73	19.46	18.56	18.62	17.67	13.44	17.33		16.95		0.00	0.00	0.11
Hy	19.80	16.77	21.73	21.42	22.08	22.09	21.81	21.63	21.96	21.83	18.91		9.62		4.48	4.04	3.99
Ol	0.00	2.42	0.00	0.00	0.00	0.00	0.00	0.00	0.00	0.00	2.00		9.96		0.00	0.00	0.00
Il	5.64	5.17	3.84	4.05	5.60	4.62	4.33	4.43	3.86	6.72	4.57		3.87		1.12	1.08	1.03
Mt	3.23	3.36	2.77	3.09	3.25	3.16	2.94	2.96	2.77	3.29	3.15		3.04		0.77	0.72	0.70
Ap	0.72	0.81	0.51	0.51	0.63	0.42	0.53	0.51	0.51	0.97	0.76		0.81		0.25	0.23	0.21
Mg#	42.9	42.5	52.1	48.1	45.0	47.8	49.9	49.6	52.0	43.5	45.5		48.4		16.8	13.9	16.6

TABLE 3. TRACE ELEMENT COMPOSITIONS OF MILL CREEK DIABASE DIKES, EASTERN ARBUCKLE MOUNTAINS

Sample (ppm)	Arb-01	Arb-09	Arb-10	Arb-11	Arb-12	Arb-13	Arb-14	Arb-22	Arb-26	Arb-29	Arb-32	Arb-34	Arb-36	Arb-37	Arb-42
Ga		22.5				20.4						21.5		18.5	18.0
V		349				310						317		352	334
Co		50.7				47.2						50.2		48.5	50.5
Ni		36				31						33		20	25
Cu		223				187						188		150	185
Zn		78				55						46		75	74
Li	8.9		9.8	16.9	10.9		19.4	15.0	42.8	10.7	15.4		26.9		
Rb	8.3	29.4	9.8	22.2	15.6	16.5	38.0	51.7	29.7	31.5	23.3	16.0	27.4	25.0	56.5
Sr	334.2	481.9	235.8	407.6	343.7	367.0	315.1	368.8	825.9	468.3	425.9	374.5	803.1	314.3	422.0
Y	26.4	27.9	26.8	23.4	21.5	22.3	28.1	42.7	24.9	24.6	29.6	23.0	27.2	29.4	25.8
Zr	118.6	131.7	131.0	125.8	115.6	113.2	138.2	176.1	166.5	123.0	156.8	127.3	171.4	140.2	141.5
Nb	8.2	12.3	11.5	20.2	11.9	10.3	16.7	22.9	41.0	11.9	20.0	11.7	36.0	19.4	24.6
Mo	2.0	1.0	1.6	1.3	1.6	1.0	1.4	1.8	1.8	1.0	1.8	1.0	1.8	1.0	1.0
Cs	0.3	2.0	0.5	1.0	0.9	0.8	2.0	1.6	0.9	2.0	0.4	1.1	0.2	0.3	0.5
Ba	188.3	317.0	217.4	408.3	161.9	173.0	247.9	491.7	654.9	351.5	441.0	174.0	578.9	271.0	385.0
La	10.71	16.30	13.85	18.68	11.64	12.80	13.43	23.76	37.62	12.23	21.02	13.20	33.77	18.00	19.40
Ce	26.36	36.20	33.02	43.32	28.82	28.60	33.79	59.09	80.33	30.91	50.57	30.10	74.78	40.60	45.30
Pr	3.88	5.15	4.59	5.66	4.13	4.16	4.67	7.93	10.09	4.38	6.86	4.30	9.39	5.53	6.16
Nd	18.54	22.40	20.89	24.38	18.94	18.20	21.56	35.49	42.38	20.54	30.51	18.80	39.65	23.40	26.30
Sm	5.08	5.60	5.20	5.52	4.84	4.40	5.55	8.79	8.29	5.07	7.02	4.70	8.02	5.00	5.30
Eu	1.84	2.37	1.67	1.88	1.64	2.01	1.79	2.27	2.59	1.60	2.45	2.07	2.44	1.63	1.71
Gd	5.68	6.00	5.50	5.28	5.10	4.99	5.90	7.07	8.34	5.19	7.07	5.22	7.57	6.43	5.80
Tb	0.87	0.89	0.86	0.80	0.75	0.76	0.94	1.12	1.13	0.81	1.03	0.78	1.08	0.89	0.85
Dy	5.34	5.35	5.38	4.78	4.55	4.49	5.63	6.89	6.37	4.98	6.19	4.55	6.21	5.71	5.07
Ho	1.05	1.11	1.08	0.94	0.87	0.89	1.14	1.39	1.19	0.98	1.18	0.93	1.18	1.11	1.03
Er	2.87	3.09	2.99	2.65	2.34	2.46	3.19	4.00	3.16	2.77	3.18	2.53	3.25	3.10	2.68
Tm	0.39	0.39	0.43	0.37	0.32	0.30	0.43	0.56	0.43	0.39	0.43	0.32	0.46	0.47	0.40
Yb	2.45	2.62	2.71	2.29	1.92	2.02	2.78	3.52	2.64	2.39	2.60	2.10	2.85	2.85	2.51
Lu	0.37	0.37	0.40	0.33	0.27	0.29	0.40	0.51	0.37	0.33	0.37	0.29	0.40	0.43	0.34
Hf	3.6	4.0	3.8	4.6	3.3	3.4	5.8	6.0	5.7	3.2	5.6	3.6	4.5	3.6	3.5
Ta	0.7	1.0	0.9	1.4	0.7	0.7	0.6	1.5	3.0	0.7	1.5	0.7	1.9	1.4	1.9
Tl	0.1	0.1	0.1	0.1	0.0	0.2	0.2	0.2	0.1	0.2	0.1	0.1	0.1	0.6	0.5
Pb	1.64	3.00	2.46	2.35	2.21	2.00	4.34	10.25	4.28	4.54	3.23	3.00	7.11	3.10	3.15
Bi	0.03	< .5	0.02	0.04	0.02	< .5	0.04	0.10	0.06	0.02	0.05	< .5	0.03	0.70	0.70
Th	0.77	1.10	1.41	1.31	0.94	0.90	1.28	3.15	2.72	0.34	1.46	0.90	2.54	1.30	1.30
U	0.24	0.30	0.41	0.34	0.25	0.20	0.35	0.88	0.70	0.17	0.39	0.20	0.62	0.40	0.40

TABLE 3.TRACE ELEMENT COMPOSITIONS OF MILL CREEK DIABASE DIKES, EASTERN ARBUCKLE MOUNTAINS, CONTINUED

Sample (ppm)	Arb-44	Arb-48	Arb-49a	Arb-49b	Arb-50	Arb-147	Arb-192	Arb-201	Arb-202	Arb-205	Arb-206	Arb-207	Arb-208	Mean Dike	Std Dev
Ga			22.2			18.8	20.4	23.0	20.6	22.5	24.8	22.1	26.3	21.5	2.3
V			358			297			278				456	339	51
Co			53.6			49.6	45.7	55.9	50.3	52.4	55.6	51.6	44.6	50.5	3.3
Ni			30			31	67	89	32	74	72	73	47	47	23
Cu			149			146			185					177	27
Zn			60			40			42					59	15
Li	47.0	35.4	54.8		9.0									23.1	15.7
Rb	30.1	15.8	17.5	17.9	17.1	13.3	15.0	20.7	16.7	14.4	17.3	13.6	24.2	22.7	11.3
Sr	411.8	371.3	377.3	396.1	371.1	378.5	196.5	366.5	357.9	384.2	387.0	386.7	343.4	400.6	130.4
Y	32.2	24.1	32.1	35.0	30.9	21.7	34.8	24.8	22.7	25.3	26.6	21.6	39.2	27.7	5.4
Zr	186.2	129.8	204.5	202.0	183.3	111.9	115.6	127.1	133.0	118.5	120.7	105.0	206.2	143.6	30.8
Nb	34.7	13.8	25.1	22.8	21.7	10.4	13.9	13.7	12.8	11.9	12.5	9.5	27.8	18.2	8.6
Mo	2.4	1.2	2.3	1.0	2.6	1.0								1.5	0.5
Cs	1.3	0.5	1.7	1.4	1.4	0.7	1.1	0.4	1.1	0.5	0.7	0.9	0.2	0.9	0.6
Ba	869.3	229.4	289.9	263.0	338.3	146.0	146.0	289.0	187.0	201.0	164.0	244.0		312.2	172.8
La	35.46	14.05	22.71	21.60	19.59	11.30	12.00	15.00	13.30	12.50	13.40	11.50	26.7	18.1	7.5
Ce	74.72	32.85	49.19	52.20	45.43	28.00	32.20	34.80	29.60	30.90	32.00	27.90	61.0	41.9	15.6
Pr	10.36	4.88	7.23	7.16	6.24	4.09	4.45	5.06	3.99	4.55	4.67	4.09	8.65	5.8	1.9
Nd	40.62	20.64	29.73	32.80	28.11	19.50	17.10	24.20	19.00	22.00	23.10	19.00	40.4	25.6	7.8
Sm	8.86	5.38	7.37	7.10	7.01	4.30	4.60	5.20	4.90	5.10	5.20	4.50	8.1	5.9	1.4
Eu	3.11	1.81	2.40	2.52	2.19	1.63	1.81	2.05	1.76	1.95	2.14	1.83	3.12	2.08	0.42
Gd	8.41	5.69	7.87	8.88	7.29	5.77	5.86	5.50	5.20	5.62	5.51	4.83	8.61	6.29	1.23
Tb	1.19	0.86	1.16	1.24	1.09	0.77	0.95	0.80	0.72	0.82	0.82	0.73	1.27	0.93	0.17
Dy	6.95	4.97	6.86	7.62	6.41	4.71	6.06	4.65	4.66	4.98	4.88	4.21	7.52	5.57	0.98
Ho	1.33	0.97	1.35	1.37	1.25	0.85	1.22	0.86	0.83	0.88	0.90	0.76	1.44	1.07	0.19
Er	3.54	2.63	3.48	3.48	3.35	2.17	3.65	2.42	2.50	2.61	2.66	2.27	4.09	2.97	0.51
Tm	0.51	0.37	0.50	0.48	0.45	0.30	0.46	0.32	0.28	0.33	0.34	0.28	0.55	0.40	0.08
Yb	3.15	2.13	3.04	2.87	2.80	1.86	2.97	2.04	2.05	2.12	2.24	1.89	3.58	2.54	0.47
Lu	0.47	0.33	0.50	0.41	0.40	0.25	0.43	0.27	0.28	0.29	0.30	0.26	0.49	0.36	0.08
Hf	5.2	3.9	6.4	5.0	5.2	2.9	3.7	3.8	3.5	3.6	3.7	3.1	6.0	4.3	1.0
Ta	1.9	0.8	1.4	1.7	1.2	0.8	0.3	1.3	0.7	1.1	0.9	0.8	2.0	1.2	0.6
Tl	0.1	0.0	0.1	0.3	0.0	0.3	0.1	0.1	0.9	0.1	0.1	0.1	0.1	0.2	0.2
Pb	5.52	2.23	4.44	3.19	2.83	2.35	2.41	2.84	2.60	2.48	2.60	2.72		3.44	1.81
Bi	0.02	0.02	0.02	0.90	0.02	0.60	0.50	0.50		0.50	0.50	0.50		0.28	0.29
Th	2.46	1.13	2.02	1.30	1.70	0.60	0.80	1.10	0.90	0.70	0.70	0.80	1.9	1.34	0.69
U	0.65	0.30	0.47	0.50	0.42	0.20	0.30	0.40	0.30	0.30	0.30	0.30	0.6	0.39	0.17

TABLE 4. TRACE ELEMENT COMPOSITIONS OF LOW-TH OLDER (?) DIABASE DIKES, EASTERN ARBUCKLE MOUNTAINS

Sample (ppm)	Arb-02	Arb-03	Arb-05	Arb-06	Arb-07	Arb-17	Arb-18	Arb-19	Arb-20	Arb-28	Arb-31	Arb-38	Arb-40
Ga	17.6							18.7					
V	249							212					
Co	55.4							52.2					
Ni	121							74					
Cu	92							71					
Zn	36							35					
Li	6.8	50.4	41.5	19.0	65.5	7.9	16.7		47.7	16.2	9.1	4.8	22.9
Rb	2.5	35.2	13.5	10.5	16.1	2.8	9.3	8.3	12.1	24.0	7.0	2.1	21.6
Sr	393.1	401.1	478.6	450.7	562.7	377.5	240.8	557.8	607.6	366.2	398.7	381.0	391.8
Y	15.7	17.7	17.9	21.8	14.1	15.0	12.8	17.6	18.1	23.9	17.3	16.9	16.7
Zr	60.1	43.2	56.0	93.8	52.2	56.1	54.0	60.4	31.5	88.9	66.2	62.3	74.8
Nb	2.5	3.7	3.7	6.2	2.8	2.4	4.3	2.4	2.7	6.6	2.7	2.8	6.5
Mo	1.0	0.9	1.0	1.0	0.6	1.3	1.7	1.0	1.1	0.8	0.9	1.4	1.1
Cs	0.2	2.7	0.5	1.5	0.8	0.2	0.6	0.7	1.2	2.3	0.8	0.0	0.5
Ba	143.6	294.4	122.6	253.4	128.3	134.1	102.0	145.0	175.8	176.3	134.1	154.7	168.5
La	4.67	6.22	6.20	11.41	4.83	4.46	4.94	4.40	4.64	10.50	5.07	5.00	8.83
Ce	12.11	16.78	17.61	28.71	13.62	11.78	11.35	12.00	12.85	26.58	13.17	12.76	21.73
Pr	1.85	2.67	2.69	4.24	2.06	1.82	1.57	1.92	2.03	3.86	1.95	1.97	3.16
Nd	9.17	13.57	13.50	20.23	10.40	9.01	7.32	10.40	10.56	18.10	9.79	9.95	15.02
Sm	2.70	3.80	3.81	5.13	2.89	2.61	1.99	2.60	3.06	4.76	2.88	2.90	3.81
Eu	1.00	1.33	1.33	1.83	1.05	0.99	0.74	1.11	1.15	1.55	1.08	1.07	1.34
Gd	3.09	4.22	4.20	5.33	3.19	3.12	2.33	3.55	3.60	5.11	3.44	3.37	4.02
Tb	0.50	0.64	0.64	0.78	0.50	0.51	0.38	0.55	0.58	0.79	0.55	0.53	0.60
Dy	3.18	3.88	3.89	4.53	2.99	3.20	2.53	3.58	3.60	4.90	3.50	3.36	3.60
Ho	0.65	0.74	0.75	0.87	0.58	0.63	0.52	0.70	0.73	0.96	0.71	0.69	0.70
Er	1.83	1.98	2.02	2.25	1.54	1.88	1.53	1.83	2.02	2.59	2.05	1.97	1.84
Tm	0.26	0.26	0.27	0.30	0.21	0.25	0.22	0.26	0.29	0.36	0.28	0.28	0.25
Yb	1.64	1.63	1.60	1.83	1.27	1.57	1.43	1.67	1.72	2.25	1.82	1.75	1.49
Lu	0.23	0.21	0.21	0.25	0.17	0.22	0.21	0.24	0.24	0.30	0.26	0.27	0.20
Hf	2.4	1.6	2.4	3.4	2.6	2.2	1.2	1.7	1.6	3.7	3.0	2.0	2.3
Ta	0.2	0.2	0.3	0.4	0.2	0.1	0.4	0.2	0.2	0.5	0.2	0.1	0.4
Tl	0.0	0.3	0.0	0.2	0.0	0.0	0.0	0.1	0.0	0.1	0.0	0.0	0.1
Pb	1.57	4.15	2.80	1.99	1.94	1.11	0.93	2.16	2.29	2.06	1.44	1.33	5.55
Bi	0.04	0.06	0.07	0.02	0.04	0.05	0.01	0.60	0.07	0.06	0.04	0.01	0.02
Th	0.14	0.18	0.17	0.44	0.15	0.12	0.41	0.10	0.20	0.64	0.14	0.12	0.47
U	0.04	0.04	0.06	0.14	0.04	0.03	0.09	0.10	0.05	0.17	0.03	0.04	0.12

TABLE 4. TRACE ELEMENT COMPOSITIONS OF LOW-TH OLDER (?) DIABASE DIKES, EASTERN ARBUCKLE MOUNTAINS, CONTINUED

Sample (ppm)	Arb-40*	Arb-46	Arb-146	Arb-170	Arb-203	Arb-204	Mean Dike	Std Dev
Ga		21.9	18.3	18.6	24.6	23.3	20.4	2.8
V		278	260				250	28
Co		56.0	56.1	53.1	62.2	56.3	55.9	3.2
Ni		79	116	147	123	106	109	26
Cu		80	92				84	10
Zn		47	38				39	5
Li	15.8						24.9	19.6
Rb	23.0	10.7	3.0	2.3	23.9	32.8	13.7	10.4
Sr	412.5	617.5	408.3	368.1	455.5	412.9	435.9	93.7
Y	17.4	30.1	18.5	17.4	20.1	22.1	18.5	3.9
Zr	77.0	127.2	63.0	48.6	75.0	91.4	67.5	21.8
Nb	6.8	5.0	2.6	2.7	4.8	4.9	4.0	1.6
Mo	0.9	1.0	1.0				1.0	0.3
Cs	0.5	0.4	0.1	0.1	0.6	0.3	0.7	0.7
Ba	184.3	357.0	142.0	136.0	184.0	369.0	184.5	77.5
La	9.32	12.00	4.50	4.30	6.90	7.90	6.64	2.57
Ce	22.98	30.30	12.00	10.40	18.00	20.00	17.09	6.29
Pr	3.36	4.64	1.89	1.71	2.83	3.09	2.59	0.92
Nd	15.74	22.10	10.00	9.00	14.30	15.70	12.84	4.14
Sm	3.98	5.00	2.60	2.50	3.70	3.80	3.40	0.90
Eu	1.41	1.88	1.10	1.08	1.62	1.59	1.28	0.31
Gd	4.19	6.76	3.79	3.15	4.16	4.36	3.95	0.99
Tb	0.62	0.98	0.57	0.50	0.63	0.64	0.60	0.13
Dy	3.75	6.10	3.87	3.04	3.80	4.14	3.76	0.79
Ho	0.71	1.16	0.73	0.62	0.67	0.77	0.73	0.14
Er	1.91	3.10	1.93	1.92	1.96	2.44	2.03	0.36
Tm	0.26	0.45	0.28	0.27	0.27	0.30	0.28	0.05
Yb	1.51	2.67	1.79	1.77	1.68	1.98	1.74	0.31
Lu	0.20	0.39	0.25	0.26	0.24	0.28	0.24	0.05
Hf	2.3	3.2	1.7	1.7	2.2	2.8	2.3	0.7
Ta	0.4	0.4	0.2	0.2	0.4	0.4	0.3	0.1
Tl	0.1	0.5	0.5	0.1	0.1	0.1	0.1	0.1
Pb	4.31	3.18	1.84	1.66	3.38	2.74	2.44	1.21
Bi	0.02	0.70	1.00	0.50	0.50	0.50	0.23	0.30
Th	0.47	0.30	0.10	0.10	0.10	0.20	0.24	0.16
U	0.12	0.30	0.10	0.10	0.10	0.10	0.09	0.06

of Texas at Dallas (UTD). Reproducibility of $^{87}Sr/^{86}Sr$ is ± 0.00004 for data reported here, which have been adjusted to correspond to a value of 0.70800 for the E&A $SrCO_3$ standard. $^{143}Nd/^{144}Nd$ ratios were also determined using the UTD Finnigan-MAT261 in the dynamic multicollector mode. Calculations of $\varepsilon_{Nd(T)}$ were made assuming Bulk Earth $^{147}Sm/^{144}Nd$ = 0.1967 and using values of ε_{Nd} for the UCSD standard (-15.2) and BCR (-0.16) (Pier et al., 1989). A total range of ± 0.00002 observed for $^{143}Nd/^{144}Nd$ of the standard (mean value = 0.511868) is taken as the analytical uncertainty for the samples. The results are summarized in Table 5.

GEOCHEMISTRY

Major Elements

All of the analyzed Mill Creek diabase dikes are compositionally similar with restricted ranges in major-element compositions (Table 2). The rocks are characterized by SiO_2 contents between 46 and 52 wt %, moderate to high TiO_2 (1.8 to 2.9 wt %), high Fe_2O_3 (12.6 to 15.5 wt %), low Al_2O_3 (13.3 to 15.7 wt %), and moderately low MgO (4.3 to 7.0 wt %). CIPW normative compositions are either olivine tholeiites or quartz tholeiites (Table 2). They also display cation-normative (Irvine and Baragar, 1971) subalkaline compositions. On a SiO_2 vs. (Na_2O + K_2O) diagram (not shown), the diabases, typical of many continental flood basalts, are transitional between subalkalic and alkalic basalts and contain 2.7 to 4.8 wt% Na_2O + K_2O.

The diabases have experienced moderate amounts of crystal fractionation from more primitive mantle melts. This is shown by whole-rock MgO compositions, Mg# (=100*Mg/Mg + Fe) from 52 to 36, <70 to 120 ppm Cr, and 20 to 90 ppm Ni. Furthermore, major- and compatible-trace element variations (not shown here) define reasonably coherent trends with MgO or Mg# that are consistent with fractional crystallization playing an important role in the compositional variation.

The diabases are further characterized by high FeO^T/MgO ratios (FeO^T as total Fe). All of the Mill Creek diabases are high-Fe tholeiites according to the classification of Arculus (2003) (Figure 5). On the FeO^T/MgO plot, they are similar to other SOA diabases in the Wichita Mountains and in the nearby subsurface (Figure 5A). Furthermore, Figure 5B shows that the high-Fe character of the Mill Creek diabases compare closely in FeO^T/MgO – SiO_2 behavior with well-known high-Ti continental flood basalt (CFB) provinces from the Columbia River, Deccan, Ethiopia, Karoo, and the Paraná regions. This strengthens our suggestion that the composition of Mill Creek diabases were feeders for an overlying LIP, which was stripped off, probably during Paleozoic uplift related to the Ouachita orogeny.

The reason or reasons of why the diabases are so fractionated (low Mg#) and Fe-rich are not clear. CFBs produced by melting during decompression plume development and lithospheric extension typically have low SiO_2 and high $Fe_2O_3^T$ (Turner and Hawkesworth, 1995). A possible senario leading to development of the Mill Creek di-

TABLE 5: ISOTOPIC COMPOSITIONS OF SR AND ND IN MILL CREEK DIABASE DIKES, EASTERN ARBUCKLE MOUNTAINS

Sample	Arb-11	Arb-26	Arb-32	Arb-48	Arb-49	Arb-147	Arb-201	Mean MC
SiO_2	46.2	46.7	48.8	49.5	49.3	50.3	47	48.3
Mg#	44.0	39.4	43.1	46.6	42.9	52.1	45.0	44.7
K_2O	0.79	1.17	0.94	0.70	0.73	0.45	0.52	0.76
Rb (ppm)	24.8	29.1	22.0	14.7	13.8	14.0	23.7	20.3
Sr (ppm)	443	882	424	363	380	360	389	463
$^{87}Rb/^{86}Sr$	0.162	0.095	0.155	0.117	0.105	0.113	0.176	0.132
Sm (ppm)	6.24	9.06	7.69	5.74	7.71	5.11	6.15	6.81
Nd (ppm)	27.2	45.1	32.7	22.3	30.9	19.4	24.4	28.9
$^{147}Sm/^{144}Nd$	0.1387	0.1214	0.1422	0.1556	0.1508	0.1592	0.1524	0.1458
$^{87}Sr/^{86}Sr$	0.70535	0.70461	0.70544	0.70481	0.70468	0.70500	0.70622	0.70516
$^{87}Sr/^{86}Sr$ (550)	0.70408	0.70387	0.70423	0.70390	0.70386	0.70412	0.70484	0.70413
$^{143}Nd/^{144}Nd$	0.51253	0.51245	0.51256	0.51269	0.51273	0.51270	0.51264	0.51261
$\varepsilon_{Nd(550)}$	2.0	1.6	2.4	4.0	5.1	3.8	3.3	3.2

abase compositions might be the presence of low oxygen fugacity in the magma source that would favor the early crystallization of Mg-silicates and delay the crystallization of plagioclase and Fe-Ti oxides. A further contributing factor may have been the dense crustal root beneath the SOA (Keller et al., 1983; Keller and Stephenson, 2007; Hanson et al., 2013) that interacted with the upwelling diabasic magma and enhanced its fractionated character. Certainly the Fe-rich nature of large volumes of SOA magmas needs to be explained.

Trace Elements

Trace-element data (Table 3) are consistent with the major element data in demonstrating tholeiitic affinities for the Mill Creek diabases. The tholeiitic character is indicated by moderate to high TiO_2 and low P_2O_5 (mainly <0.4) contents and low Nb/Y (<1) ratio. Furthermore, the diabases display a characteristic within-plate smooth incompatible-element pattern (Figure 6A) with essentially no depletion in high-field strength elements such as Nb, Ta, Zr, Hf, and Ti. The Cambrian diabases are enriched in incompatible elements compared to primitive mantle (Figure 6A) with strongly incompatible elements Nb, Ta, and the LREE being enriched by a factor of about 20 to 80. Incompatible-element plots against other normalizing parameters indicate that the diabases have enriched compositions between enriched mid-ocean ridge basalt (E-MORB) (Figure 7A) and ocean island basalt (OIB) (Figure 7B). Figure 7 also shows that the Cambrian Mill Creek diabases are distinct from their older (?) low-Th counterparts in containing greater abundances of Th, Nb, Zr, Hf, and the LREE. For example, the mean Th composition of the Mill Creek diabases is 1.34 ppm (Table 3) compared to the mean Th value of 0.24 ppm for the low-Th diabases (Table 4). The mean Th composition of the Mill Creek diabases is thus five to six times greater than the mean of the low-Th diabases. Of particular additional note is the relative depletion in Th for both the Mill Creek and the older (?) low-Th Arbuckle diabases (Figure 7). The depletion may reflect the presence of anomalously dense mantle (Keller et al., 1983; Keller and Stephenson, 2007; Hanson et al., 2013) beneath the SOA and further suggest that there was little continental crustal contamination of Mill Creek diabase magma on the basis of the trace-element data.

Figure 6B shows that the Mill Creek diabase dikes have closely similar incompatible-element compositions with the extensional Ediacaran basalt and diabase swarms of eastern North America (Puffer, 2002). Puffer demonstrates that two main episodes of extensional magmatism

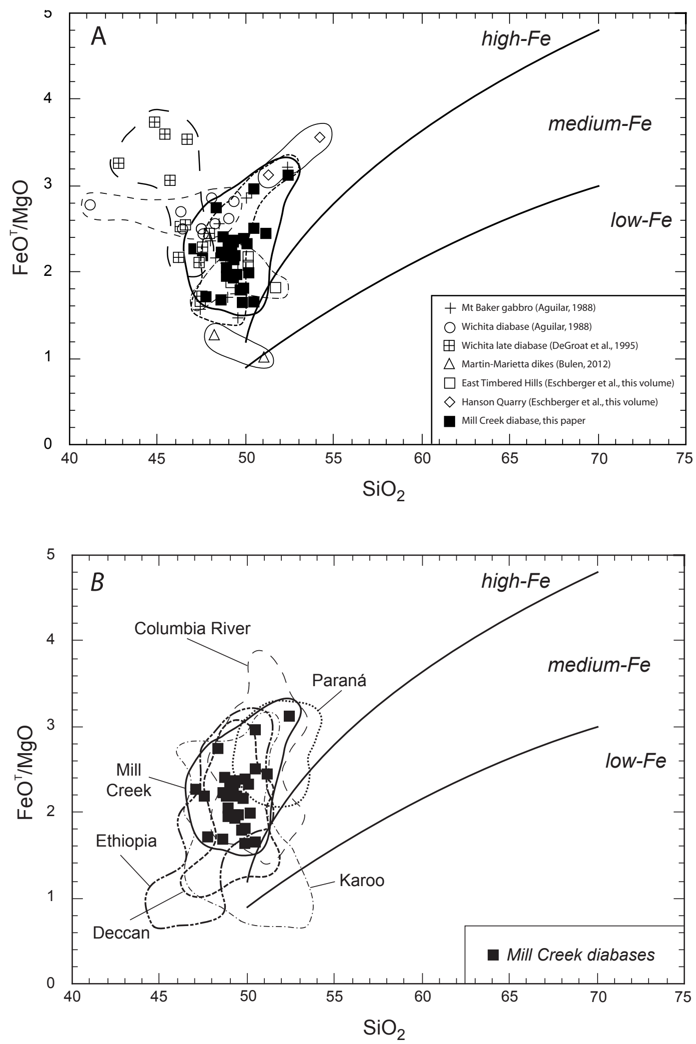

Figure 5: A) SiO_2 vs FeO^T/MgO diagram (Arculus, 2003) of Southern Oklahoma Aulacogen diabasic dikes. Sources: Mt. Baker gabbro and Wichita diabase (Aquilar, 1988); Wichita late diabase (DeGroat et al., 1995); Martin Marietta dikes (Bulen, 2012); East Timbered Hills (Eschberger et al., 2014); Hanson Quarry diabase (Eschberger and Hanson, 2014); Mill Creek diabases (this paper). B) SiO_2 vs FeO^T/MgO diagram of Mill Creek diabase compared to continental flood basalt provinces. Sources: Columbia River (Hooper and Hawkesworth, 1993), Deccan (Cox and Hawkesworth, 1985; Lightfoot et al., 1990), Ethiopia (Pik et al., 1998), Karoo (Ellam and Cox, 1991; Marsh et al., 1997), Paraná (Peate et al., 1999), Mill Creek diabases (this paper).

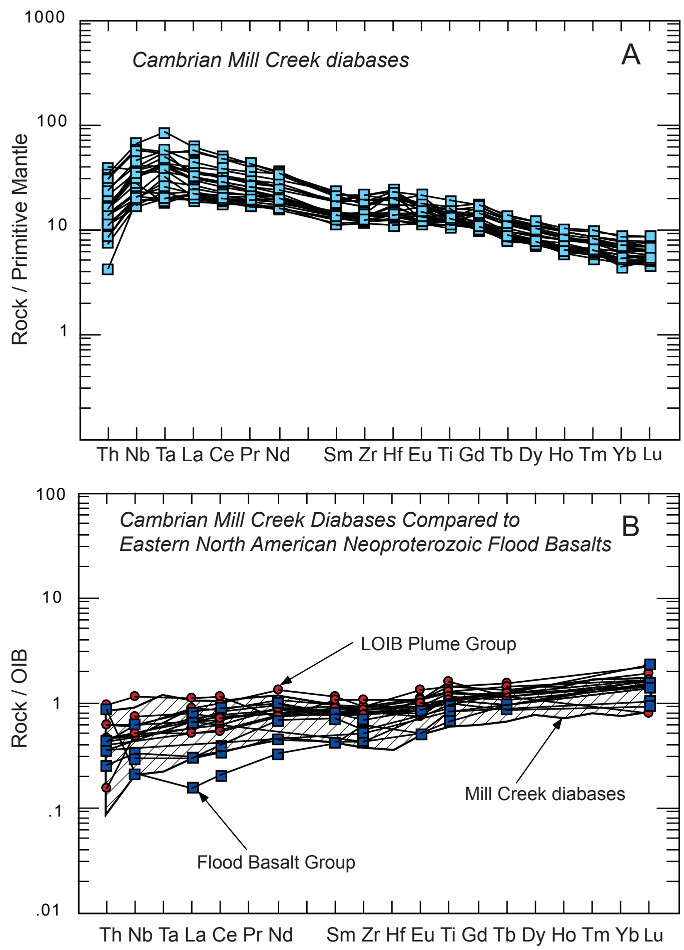

Figure 6: Normalized incompatible element patterns of Cambrian Mill Creek diabases and eastern North American Neoproterozoic basalts and diabase dikes. A) Mill Creek diabase; B) Mill Creek diabase compared to Neoproterozoic flood basalts (Puffer, 2002). OIB, Ocean Island Basalt; LOIB, Laurentian Ocean Island Basalt. Normalizing factors (Sun and McDonough, 1989).

occurred in the Appalachians – one 615 to 564 Ma (Mid Ediacaran flood basalt group) and one at about 554 to 550 Ma (Late Ediacaran Laurentian OIB plume group). These dates record initial rifting along the margin of the Laurentian craton. As noted previously, rift-related magmatism in the SOA is about 10 to 20 Ma younger. The timing and composition of the Arbuckle dikes are thus consistent with the break-up of a supercontinent along the SOA and formation of an overlying LIP in the Early Cambrian.

Further indication that the Cambrian SOA–LIP is compositionally similar to better known Mesozoic and younger LIPs is shown in Figure 8 which compares the Cambrian Mill Creek diabases with Phanerozic CFB and OIB provinces. The Cambrian dikes are indistinguishable from most of these younger provinces. The minor differences in La/Yb compared to OIB (Figure 8A) and in Th/Ta compared to CFB (Figure 8B) presumably represent the previously noted dense mantle root and absence of a significant continental crustal source beneath the SOA.

Isotopic Ratios

Sr and Nd isotopic compositions and parent-daughter ratios of seven Mill Creek quarry diabase dikes are listed in Table 5 and plotted in Figure 9. These allow initial isotopic compositions to be reconstructed. $^{87}Rb/^{86}Sr$ of all seven dikes is low (mean = 0.13) so the initial $^{87}Rb/^{86}Sr$ is insensitive to age uncertainty. Table 5 reports $^{87}Rb/^{86}Sr$ corrected for 550 Ma of radiogenic growth with observed $^{87}Rb/^{86}Sr$. Initial $^{87}Sr/^{86}Sr$ varies between 0.70387 and 0.70484. This is similar to but slightly higher than initial $^{87}Sr/^{86}Sr$ of other SOA Cambrian mafic rocks (Figure 9). $^{147}Sm/^{144}Nd$ of the seven dikes is moderately low, 0.12 to 0.16, indicating modest LREE-enrichment of these dike rocks. This low $^{147}Sm/^{144}Nd$ allows initial $^{143}Nd/^{144}Nd$ to be inferred in spite of some age uncertainty. Initial ε_{Nd} is modestly positive, +1.6 to 5.1 (Table 5), indicating a significant contribution from depleted mantle. These are broadly similar to other continental flood basalts and LIPS (Figure 9) and further support the idea that these dikes are part of an earliest Cambrian LIP and are apparently part of the hypabyssal feeder system. These isotopic compositions fall within the field defined by dominant oceanic mantle reservoirs N-MORB, HIMU, EM1 and EM2 and are also broadly similar to sub-continental lithospheric mantle (Figure 9). It is not clear whether or not there is some contamination of mantle-derived melts by Mesoproterozoic crust like that of the host Troy Granite (Figures 2, 3), but if so it must be modest because there is no systematic variation of isotopic compositions with geochemical tracers of fractionation such as Mg# or indicators of granitic continental crust such as K_2O or SiO_2 (Table 5). Figure 10 shows a simple mixing diagram of ε_{Nd} vs. K_2O contents between a low–K_2O Mill Creek diabase dike and typical Mesoproterozoic granite of the surrounding crust. It is not possible to show any mixing on this basis or to exclude <20% crustal contamination, but we see no convincing evidence of crustal contamination.

SUMMARY

• The geochemistry (major, trace, and isotopic ratios) of Cambrian Mill Creek diabases in the eastern Arbuckle

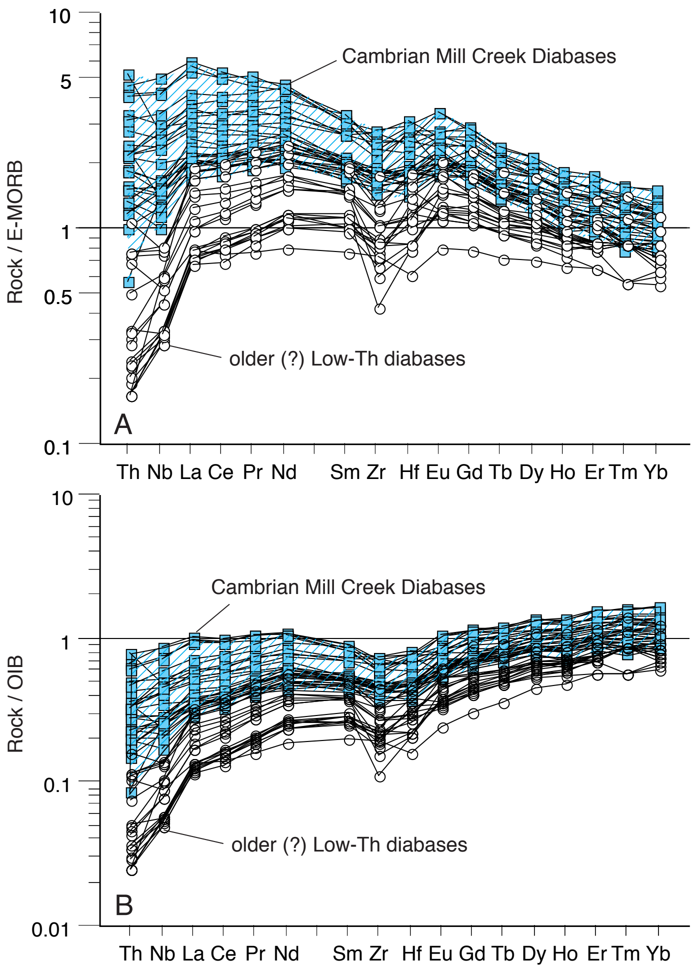

Figure 7: Normalized incompatible element patterns of Arbuckle Cambrian Mill Creek diabases and older (?) low-Th Arbuckle diabase dikes. A) normalized to E-MORB (Enriched Mid-Ocean Ridge Basalt), B) normalized to OIB (Ocean Island Basalt). Normalizing factors (Sun and McDonough, 1989).

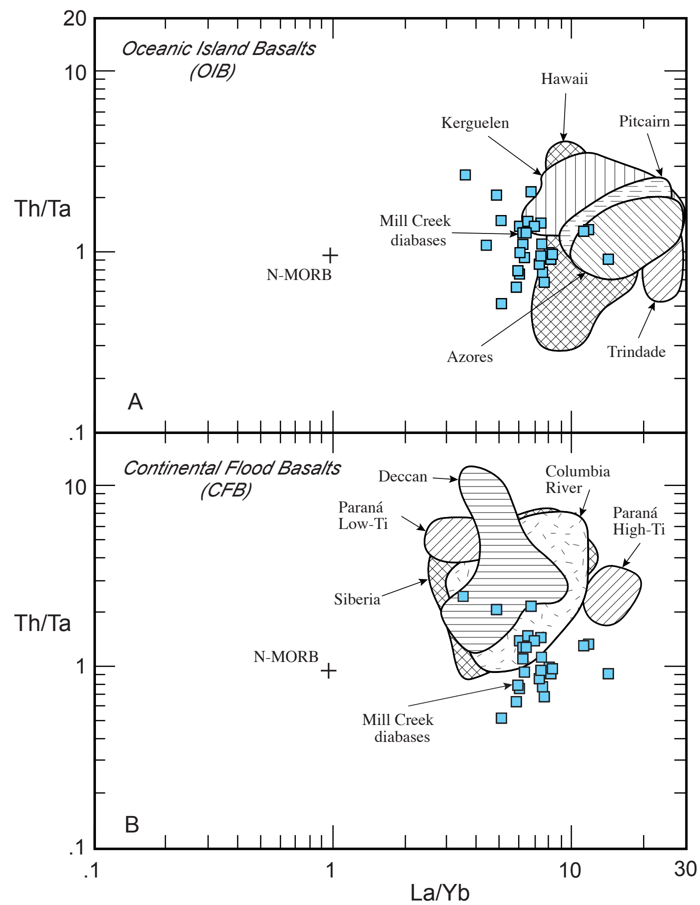

Figure 8: Cambrian Mill Creek diabase dikes compared to ocean island basalts (OIB) and continental flood basalts (CFB). Data sources: A) OIB—Azores (Turner et al., 1997), Hawaii (Frey et al., 1990), Kerguelen (Gautier et al., 1990), Pitcairn (Woodhead and Devey, 1993), Trindade (Marques et al., 1999); B) CFB—Columbia River (Hooper and Hawkesworth, 1993), Deccan (Cox and Hawkesworth, 1985; Lightfoot et al., 1990), Paraná high Ti (Peate et al., 1999), Paraná low Ti (Peate and Hawkesworth, 1996), Siberia (Lightfoot et al., 1993). N-MORB, Normal Mid-Ocean Ridge Basalt (Sun and McDonough, 1989), Mill Creek diabases (this paper).

Mountains are remarkably similar to basalts of Large Igneous Provinces (LIP).

• The apparent age and tectonic setting of Cambrian diabases are consistent with rifting and continental break-up during the Early Cambrian.

• The Cambrian diabases are the remnants of feeders to a LIP that formed over what is now the Southern Oklahoma Aulacogen (SOA).

• The Cambrian diabases show no evidence of >20% contamination by continental crust and may be free of contamination.

The Cambrian dikes thus suggest the existence of a LIP in this region and demonstrate that mafic melts associated with the Cambrian SOA–LIP were compositionally similar to better-known break-up LIPs of Mesozoic and younger age. SOA–LIP is the only evidence that we can find for a break-up LIP in southern Laurentia, but we argue that compositional similarities with other, better-preserved LIPs warrant the conclusion that the Cambrian LIP break-up of the southern mid-continent was similarly extensive. We note the abundance of felsic lavas within the SOA–LIP, a trait that differs from many other LIPs. Furthermore, the

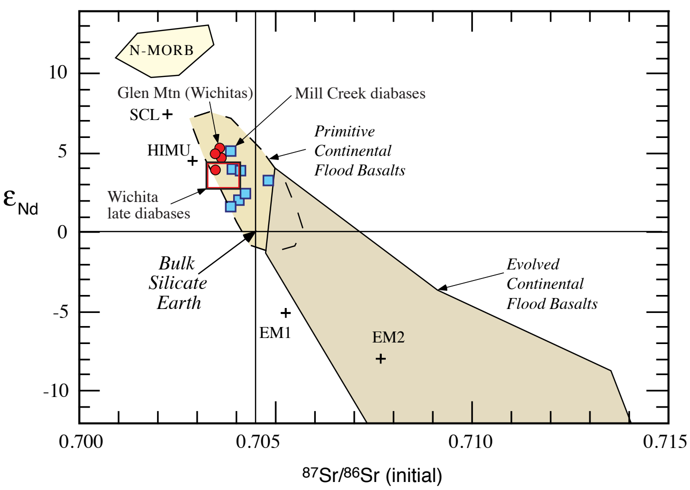

Figure 9: Initial Sr and Nd isotope plot of mafic igneous rocks, Southern Oklahoma Aulacogen. Evolved and primitive continental flood basalt boundaries (Condie, 2001). Mantle source compositions: EM1 (enriched mantle 1), EM2 (enriched mantle 2), and HIMU (high μ = high $^{238}U/^{204}Pb$) (Hart, 1984, 1988); N-MORB (Normal Mid-Ocean Ridge basalt) (Sun and McDonough, 1989). Subcontinental Lithosphere-SCL (McDonough et al., 1985). Glen Mountain Layered Series, Oklahoma (Lambert et al., 1988); Late Wichita diabase dikes, Oklahoma (Hogan et al., 1995, 1996); Mill Creek diabase dikes (this paper).

presence of a suite of west-northwest-trending microgranite porphyry dikes and a suite of apparently older diabase dikes may record a Mesoproterozoic structural grain that influenced structures throughout the Paleozoic era.

REFERENCES CITED

Aquilar, J., 1988, Geochemistry of mafic rock units of the southern Oklahoma aulacogen, southwest Oklahoma [M. S. Thesis]: Norman, Oklahoma, University of Oklahoma, 167 p.

Arculus, R. J., 2003, Use and abuse of the terms calcalkaline and calcalkalic: Journal of Petrology, v. 44, p. 929-935.

Bulen, C. L., 2012, The role of magmatism in the evolution of the Cambrian southern Oklahoma rift zone: geochemical constraints on the mafic-intermediate rocks in the Arbuckle Mountains, Oklahoma [M.S. Thesis]: Manhattan, Kansas, Kansas State University, 87 p.

Cawood, P. A., McCausland, P. J. A., and Dunning, G. R., 2001, Opening Iapetus: Constraints from the Laurentian margin in Newfoundland: Geological Society of America Bulletin, v. 113, p. 443-453.

Condie, K. C., 2001, Mantle Plumes and Their Record in Earth History, Cambridge University Press, 306 p.

Cox, K. G., and Hawkesworth, C. J., 1985, Geochemical stratigraphy of the Deccan Traps at Mahabaleshwar, Western Ghats, India, with implications for open system magmatic processes: Journal of Petrology, v. 26, p. 355-377.

DeGroat, P. J., Donovan, R. N., Hanson, R. E., and Weaver, B. L., 1995, Cambrian diabase and gabbro in the Blue Creek Canyon area, Wichita Mountains, southwestern Oklahoma: Oklahoma Geology Notes, v. 55, p. 168-186.

Denison, R. E., 1973, Basement rocks in the Arbuckle Mountains: Oklahoma Geological Survey Special Publication 73-3, p. 43-49.

Denison, R. E., 1982, Geologic cross section from the Arbuckle Mountains to the Muenster arch in southern Oklahoma and Texas: Geological Society of America Map and Chart Series MC-28R Geol. Soc. America Map and Chart Series, 8 p.

Denison, R. E., 1995, Significance of air-photograph linears in the basement rocks of the Arbuckle Mountains: Oklahoma Geological Survey Circular 97, p. 119-131.

Ellam, R. M., and Cox, K. G., 1991, An interpretation of Karoo picrite basalts in terms of interaction between asthenospheric magmas and the mantle lithosphere: Earth and Planetary Science Letters, v. 105, p. 330-342.

Eschberger, A. M., and Hanson, R. E., 2014, Igneous breccia in the West Timbered Hills, Arbuckle Mountains: origin from explosive basaltic phreatomagmatic processes: this volume.

Eschberger, A. M., Hanson, R. E., and Puckett, R. E., Jr., 2014, Carlton Rhyolite Group and diabase intrusions in the East Timbered Hills, Arbuckle Mountains: this volume.

Ewing, T. E., 1990, Tectonic Map of Texas: The University of Texas at Austin, Bureau of Economic Geology, 4 sheets, scale 1: 750,000.

Ewing, T. E., 1991, The Tectonic Framework of Texas, The University of Texas at Austin, Bureau of Economic Geology, 36 p.

Frey, F. A., Wise, W. S., Garcia, M. O., West, H., Kwon, S.-T., and Kennedy, A., 1990, Evolution of Mauna Kea Volcano, Hawaii: petrologic and geochemical constraints on postshield volcanism: Journal of Geophysical Research, v. 95, p. 1271-1300.

Gautier, I., Weis, D., Mennessier, J. P., Vidal, P., Giret, A., and Loubet, M., 1990, Petrology and geochemistry of the Kerguelen Archipelago basalts (south Indian Ocean): evolution of the mantle sources from ridge to intraplate position: Earth and Planetary Science Letters, v. 100, p. 59-76.

Gilbert, M. C., 1982, Geologic setting of the eastern Wichita Mountains with a brief discussion of unresolved problems: Oklahoma Geological Survey Guidebook 21 p. 1-30.

Gilbert, M. C., 1983, Timing and geochemistry of igneous events associated with the southern Oklahoma aulacogen: Tectonophysics, v. 94, p. 439-455.

Gilbert, M. C., and Hughes, S. S., 1986, Partial chemical characterization of Cambrian basaltic liquids of the southern Oklahoma aulacogen, *in* Gilbert, M. C., ed., Petrology of the Cambrian Wichita Mountains Igneous Suite: Norman, Oklahoma, Oklahoma Geological Survey Guidebook 23, p. 73-79.

Ham, W. E., Denison, R. E., and Merritt, C. A., 1964, Basement rock and structural evolution of southern Oklahoma: Oklahoma Geological Survey Bulletin 95, 302 p.

Hames, W. E., Hogan, J. P., and Gilbert, M. C., 1998, Revised granite-gabbro age relationships, Southern Oklahoma Aulacogen, U.S.A., *in* Hogan, J. P., and Gilbert, M. C., eds., Basement Tectonics 12: Proceedings of the Twelfth International Conference on Basement Tectonics, Kluwer, Dordrecht, The Netherlands, p. 247-249.

Hansen, W. R., and Peterman, Z. E., 1968, Basement-rock geochronology of the Black Canyon of the Gunnison, Colorado: U. S. Geological Survey Professional Paper 600C, p. C80-C90.

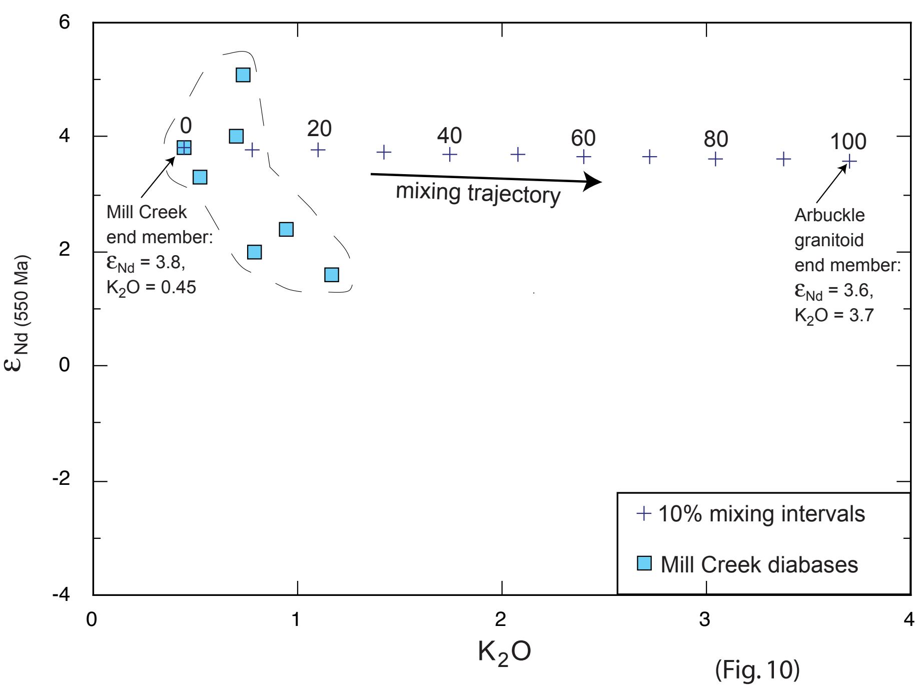

Figure 10: Langmuir mixing trajectory of K_2O vs $\varepsilon_{Nd\ (550\ Ma)}$ between Mill Creek diabase and Arbuckle granitoids. Mixing data: Mill Creek diabase (this paper): ε_{Nd} = 3.8; K_2O = 0.45. Arbuckle granitoids, ε_{Nd} = 3.6 (Rohs and Van Schmus, 2007); K_2O (unpublished, based on 55 analyses).

Hanson, R. E., Puckett, R. E., Jr., Burkholder, B. K., Eschberger, A. M., Finegan, S. A., Frazier, S. J., McCleery, D. A., Philips, C. M., and Pollard, J. B., 2011, Voluminus A-type rhyolites within a major, largely buried Cambrian rift zone in southern Oklahoma: Geological Society of America Abstracts with Programs, v. 43, p. 651.

Hanson, R. E., Puckett, R. E., Jr., Keller, G. R., Brueseke, M., Bullen, C. L., Mertzman, S. A., Finegan, S. A., and McCleery, D. A., 2013, Intraplate magmatism related to opening of the southern Iapetus Ocean: Cambrian igneous province in the southern Oklahoma rift zone: Lithos, v. 174, p. 57-70.

Harry, D. L., and Londono, J., 2004, Structure and evolution of the central Gulf of Mexico continental margin and coastal plain, southeast United States: Geological Society of America Bulletin, v. 116, p. 188-199.

Hart, S. R., 1984, A large-scale isotope anomaly in the Southern Hemisphere mantle: Nature, v. 309, p. 753-757.

Hart, S. R., 1988, Heterogeneous mantle domains: signatures, genesis, and mixing chronologies: Earth and Planetary Science Letters, v. 90, p. 273-296.

Hogan, J. P., Gilbert, M. C., Price, J. D., and Wright, J. E., 1995, Petrogenesis of A-type sheet-granites from an ancient rift. Abstract: U. S. Geological Survey Circular 1129 p. 68-69.

Hogan, J. P., Gilbert, M. C., Price, J. D., Wright, J. E., and Hames, W. E., 1996, Magmatic evolution of the southern Oklahoma aulacogen: Geological Society of America Abstracts with Programs, v. 28, p. 19.

Hogan, J. P., Price, J. D., and Gilbert, M. C., 1998, Magma traps and driving pressure: consequences for pluton shape and emplacement in an extensional regime: Journal of Structural Geology, v. 20, p. 1155-1168.

Hooper, P. R., and Hawkesworth, C. J., 1993, Isotopic and geochemical constraints on the origin and evolution of the Columbia River basalt: Journal of Petrology, v. 34, p. 1203-1246.

Irvine, T. N., and Baragar, W. R. A., 1971, A guide to the chemical classification of the common volcanic rocks: Canadian Journal of Earth Sciences, v. 8, p. 523-548.

Keller, G. R., Lidiak, E. G., Hinze, W. J., and Braile, L. W., 1983, The role of rifting in the tectonic development of the midcontinent, U. S. A.: Tectonophysics, v. 94, p. 391-412.

Keller, G. R., and Stephenson, R. A., 2007, The Southern Oklahoma and Dnieper-Donets aulacogens: a comparative analysis, *in* Hatcher, R. D., Jr., Carlson, M. P., McBride, J. H., and Martinez-Catalan, J. R., eds., 4-D Framework of Continental Crust, Geological Society of America Memoir 200, p. 127-143.

Keppie, J. D., Dostal, J., Nance, R. D., Miller, B. V., Ortega-Rivera, A., and Lee, J. K. W., 2006, Circa 546 Ma plume-related dykes in the ~1 Ga Novillo Gneiss (east-central Mexico): Evidence for the initial separation of Avolonia: Precambrian Research, v. 147, p. 342-353.

Lambert, D. D., Unruh, D. M., and Gilbert, M. C., 1988, Rb-Sr and Sm-Nd isotopic study of the Glen Mountains layered complex: Initiation of rifting within the southern Oklahoma aulacogen: Geology, v. 16, p. 13-17.

Lidiak, E. G., Denison, R. E., and Stern, R. J., 2005, Large igneous province: Cambrian diabase dikes, eastern Arbuckle Mountains, Oklahoma. Abstracts, *in* American Association of Petroleum Geologists Mid-Continent Meeting, AAPG Search & Discovery Article #90048, Oklahoma City, Oklahoma.

Lightfoot, P. C., Hawkesworth, C. J., Devey, C. W., Rogers, N. W., and Van Calsteren, P. W. C., 1990, Source and differentiation of Deccan Trap lavas: Implications of geochemical and mineral chemical variations: Journal of Petrology, v. 31, p. 1165-1200.

Lightfoot, P. C., Hawkesworth, C. J., Hergt, J., Naldrett, A. J., Gorbachev, N. S., Fedorenko, V. A., and Doherty, W., 1993, Remobilisation of the continental lithoshpere by a mantle plume: major-, trace-element, and Sr-, Nd-, and Pb-isotope evidence from picritic and tholeiitic lavas of the Noril'sk district, Siberian Trap, Russia: Contributions to Mineralogy and Petrology, v. 114, p. 171-188.

Longerich, H. P., Jenner, G. A., Fryer, B. J., and Jackson, S. E., 1990, Inductively coupled plasma-mass spectrometric analysis of geological samples: a critical evaluation based on case studies: Chemical Geology, v. 83, p. 105-118.

Marques, L. S., Ulbrich, M. N. C., Ruberti, E., and Tassinari, C. G., 1999, Petrology, geochemistry and Sr-Nd isostopes of the Trindade and Martin Vaz volcanic rocks (southern Atlantic Ocean): Journal of Volcanology and Geothermal Research, v. 93, p. 191-216.

Marsh, J. S., Hooper, P. R., Rehacek, J., Duncan, R. A., and Duncan, A. R., 1997, Stratigraphy and age of Karoo basalts of Lesotho and implications for correlations within the Karoo igneous province, *in* Mahoney, J. J., and Coffin, M. F., eds., Large Igneous Provinces: Continental, Oceanic, and Planetary Flood Volcanism: Washington,

D. C., American Geophysical Union, Geophysical Monograph 100, p. 247-272.

McDonough, W. F., McCulloch, M. T., and Sun, S.-s., 1985, Isotopic and geochemical systematics in Tertiary-Recent basalts from southeastern Australia and implications for the evolution of the sub-continental lithosphere: Geochimica et Cosmochimica Acta, v. 49, p. 2051-2067.

Olson, J. C., Marvin, R. F., and Parker, R. L., 1977, Age and tectonic setting of lower Paleozoic alkalic and mafic rocks, carbonatites, and thorium veins in south-central Colorado: U. S. Geological Survey, Journal of Research, v. 5, p. 673-687.

Peate, D. W., and Hawkesworth, C. J., 1996, Lithospheric to asthenospheric transition in low-Ti flood basalts from southern Paraná, Brazil: Chemical Geology, v. 127, p. 1-24.

Peate, D. W., Hawkesworth, C. J., Mantovani, M. M. S., Rogers, N. W., and Turner, S. P., 1999, Petrogenesis and stratigraphy of the high-Ti/Y Urubici magma type in the Paraná flood basalt province and implications for the nature of 'Dupal'-type mantle in the South Atlantic region: Journal of Petrology, v. 40, p. 451-473.

Pier, J. G., Podosek, F. A., Luhr, J. F., Brannon, J. C., and Aranda-Gomez, J. J., 1989, Spinel-lherzolite-bearing Quaternary volcanic centers in San Luis Potosi, Mexico, 2. Sr and Nd isotopic systematics: Journal of Geophysical Research, v. B94, p. 7941-7951.

Pik, R., Deniel, C., Coulon, C., Yirgu, G., Hofmann, C., and Ayalew, D., 1998, The northwestern Ethiopian plateau flood basalts: classification and spatial distribution of magma types: Journal of Volcanology and Geothermal Research, v. 81, p. 91-111.

Price, J. D., Hogan, J. P., and Gilbert, M. C., 1996, Investigations of late diabase dikes at Lake Elmer Thomas, Wichita Mountains, Oklahoma: Geological Society of America Abstracts with Programs, v. 28, p. 59.

Puckett, R. E., Jr., 2011, A thick sequence of rift-related basalts in the Arbuckle Mountains, Oklahoma, as revealed by deep drilling: Shale Shaker, January/February 2011, p. 207-217.

Puckett, R. E., Jr., Hanson, R. E., Eschberger, A. M., Bulen, C. L., and Brueseke, M., 2011, Using basement wells to investigate the subsurface Cambrian bimodal volcanic record in the southern Oklahoma aulacogen: Geological Society of America Abstracts with Programs, v. 43, p. 437.

Puffer, J. H., 2002, A late Neoproterozoic eastern Laurentian superplume: location, size, chemical composition, and environmnetal impact: American Journal of Science, v. 302, p. 1-27.

Rankin, D. W., 1976, Appalachian salients and recesses: Late Precambrian continental breakup and opening of the Iapetus Ocean: Journal of Geophysical Research, v. 81, p. 5605-5619.

Rankin, D. W., Drake, A. A., Jr., and 8-others, 1989, Pre-orogenic terranes, *in* Hatcher, R. D., Jr., Thomas, W. A., and Viele, G. W., eds., The Appalachian-Ouchita Orogen in the United States: Boulder, Colorado, Geological Society of America, v. F-2, p. 7-100.

Rohs, C. R., and Van Schmus, W. R., 2007, Isotopic connections between basement rocks exposed in the St. Francois Mountains and the Arbuckle Mountains, southern mid-continent, North America: International Journal of Earth Sciences, v. 96, p. 599-611.

Sun, S.-s., and McDonough, W. F., 1989, Chemical and isotopic systematics of oceanic basalts: implications for mantle composition and processes, *in* Saunders, A. D., and Norry, M. J., eds., Magmatism in the Ocean Basins: Oxford, United Kingdom, Geological Society Special Publication No. 42, Blackwell Scientific Publications, p. 313-345.

Taylor, C. H., 1915, Granites of Oklahoma: Oklahoma Geological Survey Bulletin 20, 108 p.

Thomas, W. A., 1989, The Appalachian-Ouachita orogen beneath the Gulf Coastal Plain between the outcrops in the Appalachian and Ouachita Mountains, *in* Hatcher, R. D., Jr., Thomas, W. A., and Viele, G. W., eds., The Appalachian-Ouchita Orogen in the United States: Boulder, Colorado, Geological Society of America, v. F-2, p. 537-553.

Thomas, W. A., 1993, Low-angle detachment geometry of the late Precambrian-Cambrian Appalachian-Ouachita rifted margin of southeastern North America: Geology, v. 21, p. 921-924.

Turner, S., and Hawkesworth, C., 1995, The nature of the sub-continental mantle: constraints from the major-element composition of continental flood basalts: Chemical Geology, v. 120, p. 295-314.

Turner, S., Hawkesworth, C., Rogers, N., and King, P., 1997, U-Th isotope disequilibria and ocean island basalt generation in the Azores: Chemical Geology, v. 139, p. 145-164.

Van Schmus, W. R., and 24 others, 1993, Transcontinental Proterozoic provinces, *in* Reed, J. C., and 6 others, ed., Precambrian: Conterminous U. S.: Boulder, Colorado, Geological Society of America, Geology of North America, v. C-2, p. 171-334.

Viele, G. W., and Thomas, W. A., 1989, Tectonic synthesis of the Ouachita orogenic belt, *in* Hatcher, R. D., Jr., Thomas, W. A., and Viele, G. W., eds., The Appalachian-Ouchita Orogen in the United States: Boulder, Colorado, Geological Society of America, v. F-2, p. 695-728.

Woodhead, J. D., and Devey, C. W., 1993, Geochemistry of the Pitcairn seamounts, I: source character and temporal trends: Earth and Planetary Science Letters, v. 116, p. 81-99.

Appendix 1: Sample Locations of Arbuckle Diabases, Eastern Arbuckle Mountains

Sample No.	Rock Unit	Rock Type	Quadrangle	Location/TR	Location/Sect
Mill Creek Diabases:					
Arb-01	Tishomingo	Diabase	Troy	03-3S-5E	NE NE SW
Arb-09	Blue River	Diabase	Wapanucka S	01-3S-8E	E NE SW NW
Arb-10	Burch	Diabase	Troy	29-3S-5E	NW NE NE NW
Arb-11	Burch	Diabase	Troy	20-3S-5E	SE NW SE SW
Arb-12	Burch	Diabase	Troy	28-2S-5E	SE SE SE SW
Arb-13	Tishomingo	Diabase	Troy	03-3S-5E	NE NE SW NE
Arb-14	Tishomingo	Diabase	Troy	03-3S-5E	NW SW SE NE
Arb-22	Burch	Diabase	Troy	17-3S-5E	NW SW SE NW
Arb-26	Burch	Diabase	Troy	08-3S-5E	NW NW SW SW
Arb-29	Burch	Diabase	Troy	20-3S-5E	NW NE NW NW
Arb-32	Tishomingo	Diabase	Reagan	28-3S-6E	NW SW SE SW
Arb-34	Burch	Diabase	Troy	07-3S-5E	NW NE SE NE
Arb-36	Tishomingo	Diabase	Reagan	20-3S-6E	NE SW SW SE
Arb-37	Tishomingo	Diabase	Reagan	20-3S-6E	SE NE SE NW
Arb-42	Tishomingo	Diabase	Reagan	24-3S-6E	NW SE SW NW
Arb-44	Troy	Diabase	Troy (quarry)	29-2S-5E	NE SW NW NW
Arb-48	Troy	Diabase	Troy (quarry)	29-2S-5E	NW SW NW NW
Arb-49a	Troy	Diabase	Troy (quarry)	29-2S-5E	NW SW NW NW
Arb-49b	Troy	Diabase	Troy (quarry)	29-2S-5E	NW SW NW NW
Arb-50	Troy	Diabase	Troy (quarry)	29-2S-5E	NW SW NW NW
Arb-147	Tishomingo	Diabase	Troy	03-3S-5E	NE SW NE
Arb-192	Tishomingo	Diabase	Reagan	28-3S-6E	C NE SW
Arb-201	Tishomingo	Diabase	Tishomingo	01-4S-5E	NE SE NE
Arb-202	Burch	Diabase	Troy	28-2S-5E	E SE SE SW
Arb-205	Burch	Diabase	Troy	29-2S-5E	NW SW NW SW
Arb-206	Burch	Diabase	Troy	09-3S-5E	N NE SW NE
Arb-207	Tishomingo	Diabase	Troy	03-3S-5E	SE SE NW SE
Arb-208	Tishomingo	Diabase	Tishomingo	01-4S-5E	SE SE NE
Older (?) Low-Th Diabases:					
Arb-02	Blue River	Diabase	Connersville NE	16-2S-7E	SE SW SW SE
Arb-03	Troy	Diabase	Troy	30-2S-5E	W SE SE NE
Arb-04	Blue River	Diabase	Wapanucka S	02-3S-8E	S SW SE NE
Arb-05	Blue River	Diabase	Wapanucka S	02-3S-8E	W SE SE NE
Arb-06	Blue River	Diabase	Boggy Depot	26-3S-9E	W NW NE NE
Arb-07	Blue River	Diabase	Wapanucka S	02-3S-8E	S SE SW NE
Arb-17	Blue River	Diabase	Connersville S	04-3S-7E	NE NW NE NE
Arb-18	Blue River	Diabase	Connersville S	04-3S-7E	NW SE NE SE
Arb-19	Blue River	Diabase	Connersville S	33-2S-7E	NE SE SW NE
Arb-20	Blue River	Diabase	Connersville S	33-2S-7E	NE NE SW SE
Arb-28	Burch	Diabase	Troy	17-3S-5E	NW NE NW NW
Arb-31	Troy	Diabase	Troy	29-3S-5E	CSL
Arb-38	Tishomingo	Diabase	Reagan	20-3S-6E	NW NE NE NE
Arb-40	Tishomingo	Diabase	Reagan	23-3S-5E	NE NE NW NE
Arb-46	Troy	Diabase	Troy	29-2S-5E	NE SW NW NW
Arb-146	Tishomingo	Diabase	Troy	03-3S-5E	C NE
Arb-170	Blue River	Diabase	Connersville NE	16-2S-7E	C SL SW SW
Arb-203	Troy	Diabase	Troy	31-2S-5E	W SE SE NE
Arb-204	Burch	Diabase	Troy	31-2S-5E	NE NE NE NE